

## Analysis Of Asymmetrical Duty-Cycle-Controlled LCL T Resonant Converter with Capacitive Output Filter

K.Bhuvaneshwari<sup>1</sup>,N.Soundiraraj<sup>2</sup>,L.Sahaya Senthamil<sup>3</sup>

PG Scholar<sup>1</sup>,Assistant Professor<sup>2</sup>,Associate Professor<sup>3</sup>,P.S.N.A CET,Dindigul.

bhuvanrkv2007@gmail.com<sup>1</sup>,soundar06@gmail.com<sup>2</sup>

**Abstract:** In many pulse width modulated DC-DC converter topologies, the controllable switches are operated in switch mode where they are required to turn the entire load current on and off during each switching cycle. Under such conditions, the switches are subjected to high switching stresses and power losses. Recently there is an increased interest in the use of resonant type DC-DC converters due to the advantages of high frequency of operation, high efficiency, small size, light weight, reduced Electro Magnetic Interference (EMI) and low component stresses. Resonant converters find applications especially in distributed energy systems like solar systems, vertical axis aero-generator and fuel cell power systems. Resonant converters are also employed in a variety of applications including power supplies for personal computers, space-craft power systems, lap-top computers, telecommunication equipments as well as DC motor drives. A series parallel resonant converter with LCL T resonant converter has been simulated and studied in this paper with open loop and closed loop operation. The proposed concept is analysed through simulation studies using MATLAB/Simulink. The simulated and experimental results shows that the output of converter is free from ripples and the converter can be used for aerospace applications.

**Keyword:** Resonant Converter, MATLAB, Electro Magnetic Interference, LCL T Resonant Converter.

### I.INTRODUCTION

The developments of the DC-DC Resonant Converters are increasing now a day due to its performance. A DC-DC Resonant Converter (RC) are used in telecommunication and aerospace application, at high frequency these converters experience high switching losses, reduced reliability, electromagnetic interference (EMI) and acoustic noise. To overcome these drawbacks, the SPRC is found to be suitable, due to various inherent advantages. The Series and parallel Resonant Converter (SRC and PRC respectively) circuits are the basic resonant converter topologies with two reactive elements. The merits of SRC include better load efficiency and inherent dc blocking of the isolation transformer due to the series capacitor in the resonant network. LCL -T Resonant converter has advantages like reduced transformer size, reduced filter size and current source characteristics. LCL-T

Voltage can be done by using a PWM rectifier at the output. While the resonant converters (RCs) have been popularly used in various other applications, such as high-frequency ac distribution system[1], fluorescent lamps[2], power factor correction[3], charging applications[4], etc., they are also shown to be a potential candidate for an application as a CC power supply due to zero-voltage switching (ZVS), zero-current switching (ZCS), high-frequency operation, high efficiency, small size, and low electromagnetic interference (EMI).

The merits of LCL-T RC are:

- 1) It is essentially output short-circuit proof. With clamp diodes, in addition, it is protected from overload operation[9].
- 2) The bridge output voltage and current are in phase. The current reduces proportionally with the load power thus maximizing full-load and part-load efficiency[5],[7],[8].
- 3) The converter lends itself for easy paralleling without any complex control for equal current sharing. Phase-shifted operation of paralleled modules reduces input and output filtering requirement[8].
- 4) The transformer leakage inductance is absorbed into the resonant network and the winding capacitance can also be gainfully utilized without losing the current-source property[11].

LCL-T RC has also been successfully applied to constant voltage power supplies[12], induction heating[13], and inductive power transfer applications[14]. Although the output current of LCL-T RC is constant irrespective of changes in the load resistance, for practical application as a current-source power supply, it should be possible to regulate the output current against input voltage variations. Some applications also demand that it should be possible to set and regulate the output current from near-zero to the maximum rated value. Since LCL-T RC behaves as a current source only when it is operated at the resonant frequency, the method using variation of switching frequency cannot be applied to control the output. Therefore, fixed frequency control methods need to be used. Clamped mode[15]-[18] or Phase

Shift Pulse Width Modulation(PSPWM) and Asymmetrical Duty Cycle PWM(ADC PWM) are the common fixed PWM control strategies.

II.ASYMMETRICAL DUTY CYCLE(ADC) PULSE WIDTH MODULATION

The CM control can be applied only with the full-bridge converter whereas ADC control can be used with half-bridge as well as full-bridge converters. While ADC control leads to asymmetric operation of the high-side and the low-side switches and leads to unequal voltages across the leg capacitors, it has been widely applied to power converters (resonant as well as non resonant) due to simpler implementation and soft switching.

III.LCL T RESONANT CONVERTER

Resonant converters use a resonant circuit for switching the transistors when they are at the zero current or zero voltage point, this reduces the stress on the switching transistors and the radio interference. To control the output voltage, resonant converters are driven with a constant pulse duration at a variable frequency. The pulse duration is required to be equal to half of the resonant period time for switching at the zero-crossing points of current or voltage. A Constant-frequency, phase-shifted operation of the primary side switches provides a convenient method for achieving zero-voltage turn-on of the switches, significantly reducing switching losses. Traditional methods utilized to achieve zero-voltage switching in full-bridge, constant-frequency PWM converters typically rely upon either the energy stored in the isolation transformer leakage inductance and/or the inclusion of a resonant inductor in series with the transformer to act as a supplemental energy storage element. This stored energy is used to charge and discharge bridge switch capacitance during a freewheeling stage created by phase shifting the “on” times of opposite pairs of transistors in the bridge configuration. Assuming sufficient energy storage, the body diode of the switch is forced into conduction before that particular device is turned on, enabling loss-less switching.

A.Circuit Description and Operation:

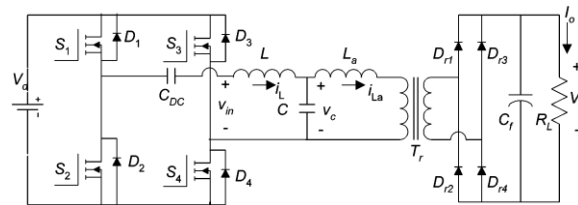


Fig 1.Circuit diagram

The circuit diagram of the full-bridge LCL-T RC is shown in Fig.1, Wherein MOSFET switches S<sub>1</sub>–S<sub>4</sub> and their body-drain diodes D<sub>1</sub>–D<sub>4</sub>, respectively, constitute the full-bridge square-wave inverter. A diode rectifier (D<sub>r1</sub>– D<sub>r4</sub>) and filter capacitor (C<sub>f</sub>) convert high-frequency ac to output dc. A dc blocking capacitor C<sub>dc</sub> is required in the full-bridge circuit to block the dc component in voltage v<sub>AB</sub> at the bridge output. At the output port of the resonant network, an isolation transformer matches the required output voltage V<sub>o</sub> and current I<sub>o</sub> to the input dc voltage.

Assuming the turns ratio (N<sub>1</sub>/N<sub>2</sub>) of isolation transformer T<sub>r</sub> to be unity, the current gain (H) and voltage gain (M) are given by,

$$H = I_o / (V_d / Z_n)$$

$$H = \frac{1}{1/Q(\omega n^2) + j\pi^2/8[(1+\gamma)\omega n - \omega_n^3]} \tag{1}$$

$$M = V_o / V_d$$

$$M = \frac{1}{(1 - \omega_n^2) + j\pi^2/8Q[(1+\gamma)\omega_n - \gamma\omega_n^3]} \tag{2}$$

Where  $\omega_o = 1/(\sqrt{LC})$ ,  $\omega n = \omega/\omega_o$ ,  $Z_n = \sqrt{L/C}$ ,  $Q = \omega_o L/R_L = Z_n/R_L$ , and  $\gamma = L_a/L$

We see from (1) that the load current is independent of load if operated at  $\omega_n = 1$  and

$$H(\omega_n = 1) = \frac{8}{\pi^2}$$

Thus, the LCL-T RC behaves as a constant-current source when operated at  $\omega_n = 1$ , if the input voltage is constant.

**B. Modes Of Operation:**

**Mode I:**

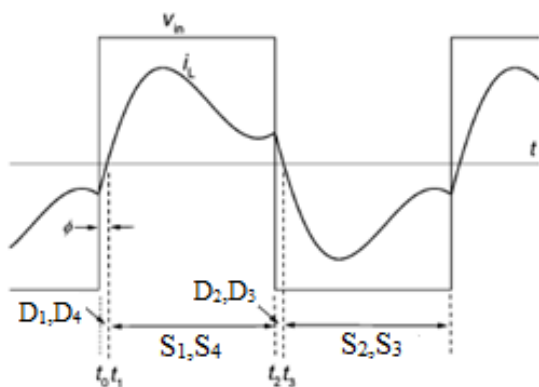


Fig 2. Mode 1

This mode of operation mainly occurs when  $D \approx 0.5$ . Before  $t = t_0$ , switches  $S_2, S_3$  were conducting. At  $t = t_0$ ,  $S_2, S_3$  are turned off and a gate pulse is applied to  $S_1, S_4$ . Since  $i_L$  is negative at this instant, it flows through  $D_1, D_4$ . At  $t = t_1$ ,  $D_1, D_4$  turns off naturally at zero current and  $i_L$  now flows through  $S_1, S_4$ . Similarly in the next half cycle,  $S_1, S_4$  are turned off at  $t = t_2$  and a gate pulse is applied to  $S_2, S_3$ . Since  $i_L$  is positive at this instant, it flows through  $D_2, D_3$ . At  $t = t_3$ ,  $D_2, D_3$  turns off naturally at zero current and  $i_L$  flows through  $S_2, S_3$ . At  $t = t_4$ ,  $S_2, S_3$  are turned off and  $S_1, S_4$  are turned on once again marking the beginning of the next cycle. Thus, in this mode, the device conduction sequence is such that the antiparallel diodes conduct prior to the switch conduction resulting in ZVS turn-on for both the switches.

**Mode II:**

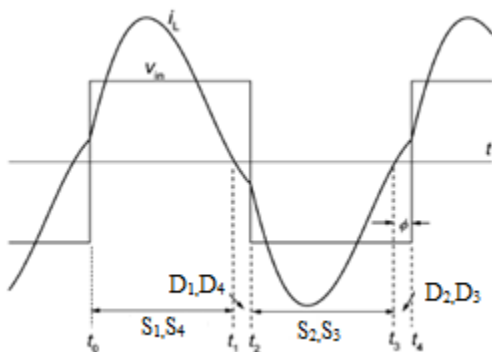


Fig 3. Mode 2

This mode of operation can also occur when  $D \approx 0.5$ . Before  $t = t_0$ , diode  $D_2, D_3$  were conducting. At  $t = t_0$ , a gate pulse is applied to  $S_1, S_4$ . Diode  $D_2, D_3$  turns

off and  $i_L$  flows through  $S_1, S_4$ . At  $t = t_1$ ,  $i_L$  reverses its direction and becomes negative.  $S_1, S_4$  turns off at zero current and  $i_L$  is transferred to  $D_1, D_4$  until  $t = t_2$  when gate pulse is applied to  $S_2, S_3$ . At this instant, diode  $D_1, D_4$  turns off and  $i_L$  is carried by  $S_2, S_3$ . At  $t = t_3$ ,  $S_2, S_3$  is turned off naturally with zero current as  $i_L$  reverses its direction and starts flowing through  $D_2, D_3$ . At  $t = t_4$ ,  $S_1, S_4$  is turned on once again marking the beginning of the next cycle. Thus, in this mode, the device conduction sequence is such that the antiparallel diodes conduct after the switch conduction resulting in ZCS turn-off for both the switches.

**Mode III:**

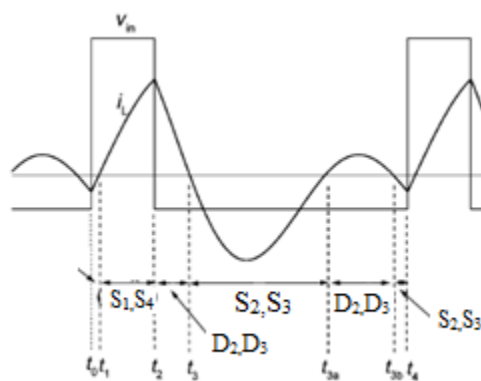


Fig 4. Mode 3

Similar to Mode I, the device conduction sequence in Mode III results in ZVS turn-on of all the switches. The difference is that  $i_L$  oscillates across zero twice during the time interval between  $t = t_2$  and  $t = t_4$  causing  $S_2, S_3$  and  $D_2, D_3$  to conduct twice during this interval. At  $t = t_2$ ,  $S_1, S_4$  are turned off and a gate pulse is applied to  $S_2, S_3$ . Since  $i_L$  is positive at this instant, it flows through  $D_2, D_3$  until  $t = t_3$  when it reverses and starts flowing through  $S_2, S_3$ . Current  $i_L$  reverses its direction at  $t = t_{3a}$  causing  $D_2, D_3$  to conduct and once again at  $t = t_{3b}$  causing  $S_2, S_3$  to conduct. The additional commutations of  $S_2, S_3$  and  $D_2, D_3$  in this mode of operation are ideally lossless since they occur under zero-current and zero-voltage condition. At  $t = t_4$ ,  $S_1, S_4$  are turned on once again marking the beginning of the next cycle.

Mode IV:

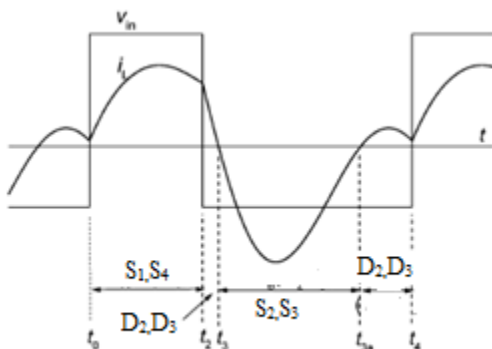


Fig 5. Mode 4

Before  $t = t_0$ , diode  $D_2, D_3$  was conducting. At  $t = t_0$ , switch  $S_1, S_4$  are turned on, which turns  $D_2, D_3$  off. The current  $i_L$  flows through  $S_1, S_4$  until  $t = t_2$  when it is turned off and a gate pulse is applied to  $S_2, S_3$ . Since  $i_L$  is positive at this instant, it flows through  $D_2, D_3$ . At  $t = t_2$ ,  $D_2, D_3$  turns off naturally at zero current and  $i_L$  now flows through  $S_2, S_3$ . At  $t = t_3a$ ,  $i_L$  reverses direction once again causing  $D_2, D_3$  to conduct until  $t = t_4$  when  $S_1, S_4$  are turned on marking the beginning of the next cycle. As compared to Mode II, in Mode IV,  $i_L$  does not reverse its direction while a gate pulse is applied to  $S_1, S_4$ . This causes  $D_2, D_3$  to conduct twice during the time interval  $t = t_2$  to  $t = t_4$ . Also, diode  $D_1, D_4$  never conducts in this mode. Observe that  $D_2, D_3$  conducts prior to the conduction of  $S_2, S_3$ , resulting in ZVS turn-on condition for  $S_2, S_3$ . However,  $S_1, S_4$  operates under hard-switching condition.

*C.State space modeling of LCL T resonant converter*

The equivalent circuit of LCL-T SPRC is shown in Fig.6. The mathematical modeling using state space technique can be obtained assuming all the components to be ideal

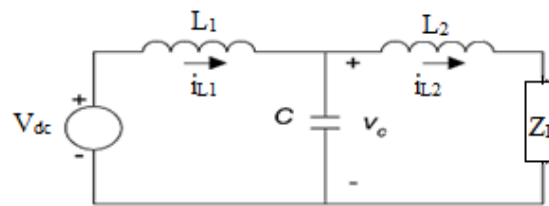


Fig.6.Equivalent Circuit Model of LCL T SPRC.

The Transfer Function for the LCL-T SPRC is given below from fig.6

$$\frac{V_0(S)}{V_i(S)} = \frac{Z_L}{L_1 L_2 C S^3 + L_1 Z_L C S^2 + (L_1 + L_2) S + Z_L} \tag{1}$$

The State Space model for LCL-T SPRC find from the equation (1)

$$\frac{Y_0(s)}{u_i(s)} = \frac{Z_L}{L_1 L_2 C S^3 + L_1 Z_L C S^2 + (L_1 + L_2) S + Z_L} \tag{2}$$

Taking inverse laplace transform and the state space equations are

$$\begin{aligned} \dot{X}_1 &= x_1 \\ \dot{X}_2 &= x_3 \\ \dot{X}_3 &= \frac{-Z_L}{CL_1L_2} x_1 - \left( \frac{L_1}{CL_1L_2} + \frac{L_2}{CL_1L_2} \right) x_2 - \frac{L_1Z_L}{L_1L_2} x_3 + \frac{Z_L}{CL_1L_2} u_i(s) \end{aligned}$$

The State Space model for LCL-T SPRC is

$$\begin{bmatrix} \dot{X}_1 \\ \dot{X}_2 \\ \dot{X}_3 \end{bmatrix} = \begin{bmatrix} 0 & 1 & 0 \\ 0 & 0 & 1 \\ -\frac{Z_L}{CL_1L_2} & -\frac{1}{CL_2} - \frac{1}{CL_1} & -\frac{Z_L}{L_2} \end{bmatrix} \begin{bmatrix} x_1 \\ x_2 \\ x_3 \end{bmatrix} + \begin{bmatrix} 0 \\ 0 \\ \frac{Z_L}{CL_1L_2} \end{bmatrix} [u_i(s)] \tag{3}$$

The output equation is,

$$Y_0 = \begin{bmatrix} 1 & 0 & 0 \\ 0 & 0 & 0 \\ 0 & 0 & 0 \end{bmatrix} \begin{bmatrix} x_1 \\ x_2 \\ x_3 \end{bmatrix} \tag{4}$$

IV.SIMULATION STUDY

The validation of the system performance is done for various regions viz. load variations, steady state region and also components variations. Simulations has been performed on the LCL T Resonant circuit with open loop and closed loop. The performance of the LCL T RC Matlab/Simulink simulation model is depicted in Fig. 7. Asymmetrical Duty Cycle PWM is

implemented in LCL T RC. During device switching, all switches operated as ZVS and ZCS condition are evaluated in Matlab/Simulink. Thus the switching losses reduced.

**SIMULATION MODEL OF LCL T RC WITH OPEN LOOP**

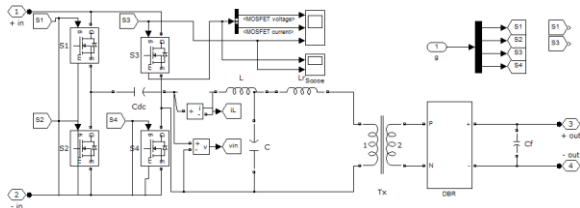


Fig 7. Simulation Diagram For LCL T RC

**SUBSYSTEM OF LCL T RC WITH OPEN LOOP**

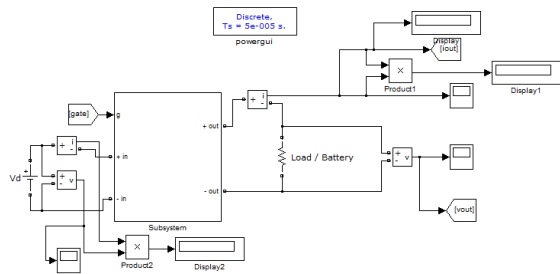


Fig 8. Subsystem Diagram

**SIMULATION MODEL FOR ADC PWM GENERATION**

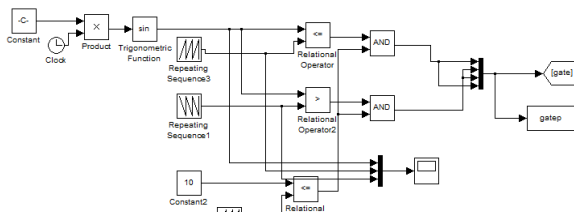


Fig 9. ADC PWM Generation

**ADC PWM SIGNAL GENERATION**

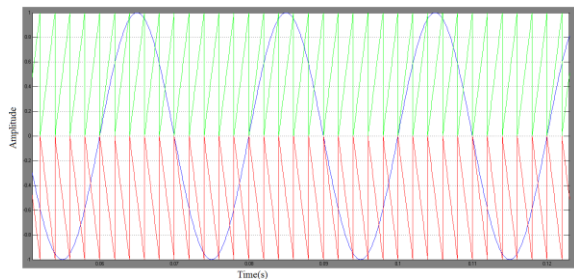


Fig 10. ADC PWM

**ZERO VOLTAGE SWITCHING & ZERO CURRENT SWITCHING**

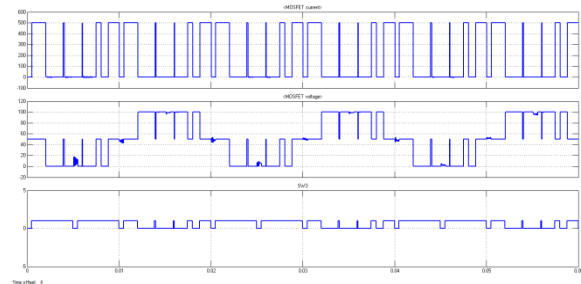


Fig 11. Simulated Output Response of ZVS, ZCS waveform of LCL-T Resonant Converter

**OUTPUT VOLTAGE & CURRENT OF LCL T RESONANT CONVERTER**

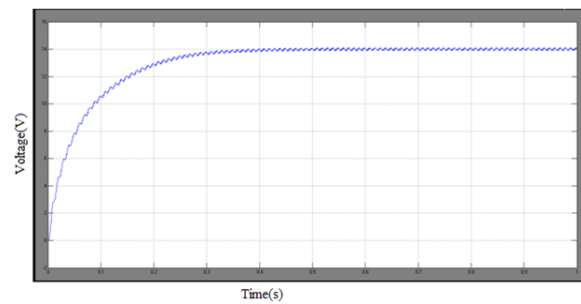


Fig 12. Output Voltage response of LCL-T Resonant Converter

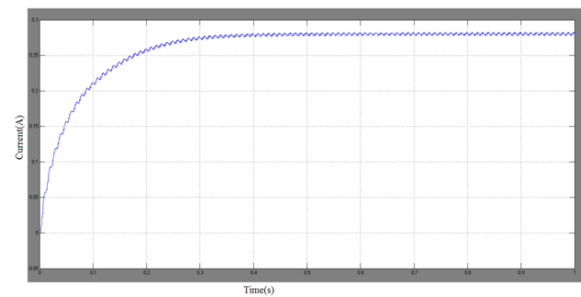


Fig 13. Output current response of LCL-T Resonant Converter

## SIMULATION MODEL FOR LCL T RC USING PI CONTROLLER

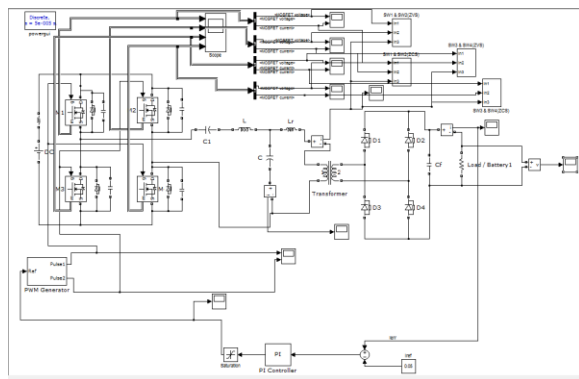


Fig 14. Simulation Diagram For LCL T RC PI Controller

## OUTPUT VOLTAGE & CURRENT OF CLOSED LOOP LCL T RC WITH LOAD VARIATIONS

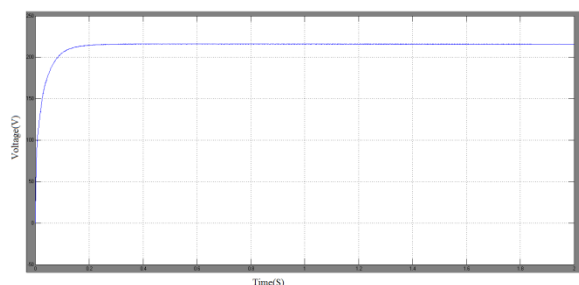


Fig 15. Output voltage response of LCL-T Resonant Converter with PI Controller

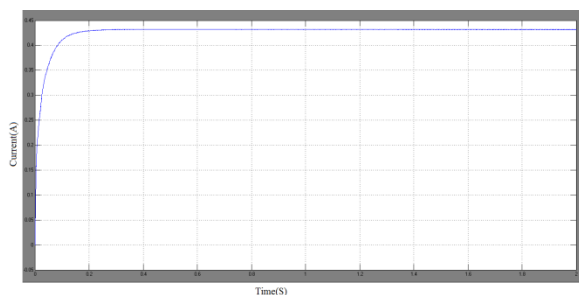


Fig 16. Output current response of LCL-T Resonant Converter with PI Controller

## CAPACITOR OUTPUT CURRENT

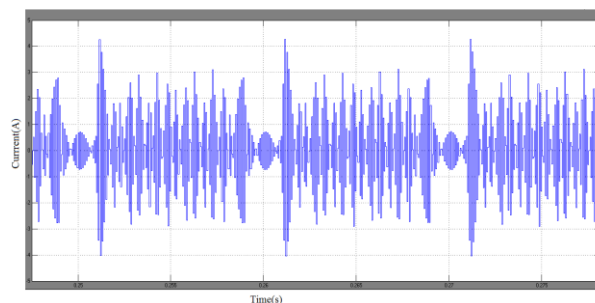


Fig 17. Capacitor output current of LCL-T Resonant Converter with PI Controller

## IV. CONCLUSION

The LCL-T RC has studied by solving the state-space model of the converter. Four distinct operating modes are identified having different circuit waveforms representing different device conduction sequences, thereby creating different conditions during device switching. Then all switches operated as ZVS and ZCS condition and thereby reducing the switching losses. This paper has successfully demonstrated the analysis, and suitability of asymmetrical duty cycle controlled (ADC) PWM of LCL T Resonant converter. The simulation based performance analysis of LCL T Resonant converter circuit has been presented along with its state space averaged model and the comparative study of LCL T RC (open loop and closed loop) with and without PI controller is presented. It is observed that ADC PWM control allows ZVS and ZCS operation over a wider range than CM control.

## REFERENCES

- [1] Z. Ye, J. C. W. Lam, P. K. Jain, and P. C. Sen, "A robust one-cycle controlled full-bridge series-parallel resonant inverter for a high-frequency AC (HFAC) distribution system," *IEEE Trans. Power Electron.*, vol. 22, no. 6, pp. 2331–2343, Nov. 2007.
- [2] T.-J. Liang, R.-Y. Chen, and J.-F. Chen, "Current-fed parallel-resonant DC-AC inverter for cold-cathode fluorescent lamps with zero-current switching," *IEEE Trans. Power Electron.*, vol. 23, no. 4, pp. 2206–2210, Jul. 2008.
- [3] M. S. Agamy and P. K. Jain, "A variable frequency phase-shift modulated three-level resonant single-stage power factor correction converter," *IEEE Trans. Power Electron.*, vol. 23, no. 5, pp. 2290–2300, Sep. 2008.
- [4] D. Fu, F. C. Lee, Y. Qiu, and F. Wang, "A novel high-power-density three-level LCC resonant converter with constant-power-factor-control for

- charging applications,” *IEEE Trans. Power Electron.*, vol. 23, no. 5, pp. 2411–2420, Sep. 2008.
- [5] H. Pollock, “Simple constant frequency constant current load-resonant power supply under variable load conditions,” *Inst. Electr. Eng. Electron. Lett.*, vol. 33, no. 18, pp. 1505–1506, Aug. 1997.
- [6] H. Seidel, “A high power factor tuned class D converter,” in *Proc. IEEE PESC 1988*, pp. 1038–1042.
- [7] H. Irie and H. Yamana, “Immittance converter suitable for power electronics,” *Trans. Inst. Electr. Eng. Jpn.*, vol. 117D, no. 8, pp. 962–969, 1997.
- [8] M. Borage, S. Tiwari, and S. Kotaiah, “Analysis and design of LCL-T resonant converter as a constant-current power supply,” *IEEE Trans. Ind. Electron.*, vol. 52, no. 6, pp. 1547–1554, Dec. 2005.
- [9] M. Borage, S. Tiwari, and S. Kotaiah, “LCL-T resonant converter with clamp diodes: A novel constant-current power supply with inherent constant-voltage limit,” *IEEE Trans. Ind. Electron.*, vol. 54, no. 2, pp. 741–746, Apr. 2007.
- [10] M. Borage, S. Tiwari, and S. Kotaiah, “A constant-current, constant voltage half-bridge resonant power supply for capacitor charging,” *Pro Inst. Electr. Eng. Electr. Power. Appl.*, vol. 153, no. 3, pp. 343–347, May 2006.
- [11] M. Borage, K. V. Nagesh, M. S. Bhatia, and S. Tiwari, “Design of LCL-T resonant converter including the effect of transformer winding capacitance,” *IEEE Trans. Ind. Electron.*, vol. 56, no. 5, pp. 1420–1427, May 2009.
- [12] C. Chakraborty, M. Ishida, and T. Hori, “Performance and design of an LCL converter for voltage regulator type applications,” *Trans. Inst. Electr. Eng. Jpn.*, vol. 119-D, no. 6, pp. 848–856, Jun. 1999.
- [13] S. Dieckerhoff, M. Ryan, and R. Doncker, “Design of an IGBT-based LCL-resonant inverter for high frequency induction heating,” in *Proc IEEE Ind. Appl. Soc. Annu. Meeting*, 1999, pp. 2039–2045.
- [14] C. Wang, G. A. Covic, and O. H. Stielau, “Investigating an LCL load resonant inverter for inductive power transfer applications,” *IEEE Trans. Power Electron.*, vol. 19, no. 4, pp. 995–1002, Jul. 2004.
- [15] F. Tsai, Y. J. Sabate, and F. Lee, “Constant frequency clamped mode resonant converters,” *IEEE Trans. Power Electron.*, vol. 3, no. 4, pp. 460–473, Oct. 1988.
- [16] F. Tsai, Y. Chin, and F. Lee, “State plane analysis of a constant frequency clamped mode parallel resonant converter,” *IEEE Trans. Power Electron.*, vol. 3, no. 3, pp. 364–377, Jul. 1988.
- [17] J. Sabate and F. C. Lee, “Off-line application of the fixed-frequency clamped-mode series resonant converters,” *IEEE Trans. Power Electron.*, vol. 6, no. 1, pp. 39–47, Jan. 1991.
- [18] J. S. Glaser, A. F. Witulsk, and R. G. Myers, “Steady-state analysis of constant frequency clamped series resonant converter,” *IEEE Trans. Aerosp. Electron. Syst.*, vol. 30, no. 1, pp. 135–143, Jan. 1994.
- [19] P. Jain, A. Martin, and G. Edwards, “Asymmetrical pulse-width-modulated resonant DC–DC converter topologies,” *IEEE Trans. Power Electron.*, vol. 11, no. 3, pp. 413–422, May 1996.
- [20] S. Mangat, M. Qui, and P. Jain, “Modified asymmetrical pulse width modulated resonant dc–dc converter topology,” *IEEE Trans. Power Electron.*, vol. 19, no. 1, pp. 104–111, Jan. 2004.
- [21] M. Qiu, P. K. Jain, and H. Zhang, “An APWM resonant inverter topology for high frequency AC power distribution systems,” *IEEE Trans. Power Electron.*, vol. 19, no. 1, pp. 121–129, Jan. 2004.
- [22] D. Tschirhart and P. Jain, “A CLL resonant asymmetrical pulsewidthmodulated converter with improved efficiency,” *IEEE Trans. Power Electron.*, vol. 55, no. 1, pp. 114–122, Jan. 2008.

